

## Effect of anharmonicity on the thermal conductivity of amorphous silica

Xueyan Zhu<sup>1,2,\*</sup> and Cheng Shao<sup>3,4,†</sup>

<sup>1</sup>*CAEP Software Center for High Performance Numerical Simulation, Beijing 100088, China*

<sup>2</sup>*Institute of Applied Physics and Computational Mathematics, Beijing 100088, China*

<sup>3</sup>*Thermal Science Research Center, Shandong Institute of Advanced Technology, Jinan, Shandong Province 250103, China*

<sup>4</sup>*Department of Mechanical Engineering, The University of Tokyo, 7-3-1 Hongo, Bunkyo, Tokyo 113-8656, Japan*



(Received 19 April 2022; revised 28 June 2022; accepted 29 June 2022; published 12 July 2022)

Proper consideration of anharmonicity is important for the calculation of thermal conductivity. However, how the anharmonicity influences the thermal conduction in amorphous materials is still an open question. In this work, we uncover the role of anharmonicity on the thermal conductivity of amorphous silica ( $a\text{-SiO}_2$ ) by comparing the thermal conductivity predicted from the harmonic theory and the anharmonic theory. Moreover, we explore the effect of anharmonicity-induced frequency shift on the prediction of thermal conductivity. It is found that the thermal conductivity calculated by the recently developed anharmonic theory (quasi-harmonic Green-Kubo approximation) is higher than that calculated by the harmonic theory developed by Allen and Feldman. The use of anharmonic vibrational frequencies also leads to a higher thermal conductivity compared with that calculated using harmonic vibrational frequencies. The anharmonicity-induced frequency shift is a mechanism for the positive temperature dependence of the thermal conductivity of  $a\text{-SiO}_2$  at higher temperatures. Further investigation on the mode diffusivity suggests that although anharmonicity has a larger influence on locons than diffusons, the increase in thermal conductivity due to anharmonicity is mainly contributed by the anharmonicity-induced increase of the diffusivity of diffusons. Finally, it is found that the cross-correlations between diffusons and diffusons contribute most to the thermal conductivity of  $a\text{-SiO}_2$ , and the locons contribute to the thermal conductivity mainly through collaboration with diffusons. These results offer new insights into the nature of the thermal conduction in  $a\text{-SiO}_2$ .

DOI: [10.1103/PhysRevB.106.014305](https://doi.org/10.1103/PhysRevB.106.014305)

### I. INTRODUCTION

The role of anharmonicity on thermal conduction in amorphous solids is quite different from that in their crystalline counterparts [1,2]. For crystalline materials, it is known that anharmonicity leads to a reduction of the phonon mean free path, which causes a decrease in thermal conductivities at higher temperatures [1]. However, for amorphous materials, thermal conductivities increase monotonically with an increase in temperature [2]. The mechanism for this phenomenon and the effect of anharmonicity on thermal conduction in amorphous materials are still open issues [3–8].

Early studies by Alexander *et al.* [3,4] and Jagannathan *et al.* [5] suggested that anharmonic interactions in amorphous materials can induce phonon-assisted hopping of localized fractons, thus leading to an increase in thermal conductivity. Allen and Feldman [6,7] derived a thermal conductivity model (AF theory) for amorphous harmonic solids from the Kubo formula. This harmonic theory has successfully predicted the positive temperature dependence of thermal conductivity in amorphous silicon [7], which is totally attributed to the increase in heat capacity with temperature. However, later studies by Shenogin *et al.* [8] showed that positive tem-

perature dependence of thermal conductivity in amorphous silica ( $a\text{-SiO}_2$ ) and polystyrene can be predicted by molecular dynamics (MD) simulations that ignore the temperature dependence of the specific heat. Their results suggest that anharmonicity is a mechanism for the rise of thermal conductivity in amorphous materials with a complex composition at higher temperatures [8]. Although current research found a positive role of anharmonicity on heat conduction in amorphous materials [3–5,8], the underlying mechanism for the influence of anharmonicity is still unclear.

Recently, several thermal conductivity models that can consider both anharmonicity and disorder have been proposed [9–12] that provide tools for investigating the effect of anharmonicity on thermal transport in amorphous materials. Lv and Henry [9] developed the Green-Kubo Modal Analysis (GKMA) method, which combines the Green-Kubo (GK) formula with lattice dynamics formalism. This method [9] uses MD simulations to obtain the modal contributions to the heat flux, thus naturally including anharmonicity and disorder. The ability to consider modal contributions allows it to apply a quantum correction to the heat capacity [9]. GKMA has been used to explore the effect of anharmonicity on the thermal conduction in  $a\text{-SiO}_2$  [10]. It was found that locons are largely responsible for the rise in thermal conductivity above room temperature, and may contribute to the thermal conductivity through collaboration with other modes due to anharmonicity [10]. Simoncelli *et al.* [11] derived an

\*zhu\_xueyan@iapcm.ac.cn

†shaocheng16@gmail.com

equation that accounts for both anharmonicity and disorder from the Wigner phase space formulation of quantum mechanics. This equation [11] can reduce to the expression derived by Peierls-Boltzmann transport equation for anharmonic crystals and AF theory for harmonic amorphous materials. Isaeva *et al.* [12] obtained an equation that can also consider both anharmonicity and disorder through combining the GK theory and a quasi-harmonic description of lattice vibrations. This equation [12] was dubbed the quasi-harmonic Green-Kubo approximation (QHGK) for thermal conductivity.

In this work, we uncover the role of anharmonicity on the thermal conduction in  $a\text{-SiO}_2$  through comparing the thermal conductivities calculated by the harmonic theory (AF theory) and the anharmonic theory (QHGK), and by investigating the effect of anharmonicity-induced frequency shift on the prediction of thermal conductivities. Moreover, mode diffusivities with and without considering anharmonicity are calculated and compared to reveal the effect of anharmonicity on diffusions and locons, respectively.

The rest of this article is organized as follows. The theoretical formulations used in this work are reviewed in Sec. II. The computational details are presented in Sec. III. The calculated vibrational mode properties are presented in Sec. IV, including the inverse participation ratio (IPR), the phonon density of states (DOS), the vibrational frequencies, and the mode lifetimes at different temperatures. The comparisons between the thermal conductivities and diffusivities calculated using QHGK and AF theory are presented in Sec. V. The effects of anharmonic vibrational frequencies on the thermal conductivities and diffusivities are investigated in Sec. VI. The conclusions are presented in Sec. VII.

## II. THEORETICAL FORMULATIONS

Two theories are used in this work to uncover the role of anharmonicity on thermal conduction in  $a\text{-SiO}_2$ , including AF theory [6] and QHGK [12]. AF theory [6] was derived based on the Kubo formula using a harmonic heat current operator. QHGK [12] was derived based on the Green-Kubo formula starting from the harmonic heat flux, and then anharmonicity was introduced through the linewidths of the vibrational normal modes when calculating the heat flux autocorrelation function.

The formula of AF theory [6] is expressed by

$$k = \frac{1}{V} \sum_i C_i(T) D_i, \quad (1)$$

where  $V$  is the volume of the system,  $C_i(T)$  is the specific heat capacity of mode  $i$ , and  $D_i$  is the mode diffusivity. The specific heat capacity of mode  $i$  is calculated by

$$C_i = k_B \frac{[\hbar\omega_i/(k_B T)]^2 e^{\hbar\omega_i/(k_B T)}}{[e^{\hbar\omega_i/(k_B T)} - 1]^2}, \quad (2)$$

where  $\omega_i$  is the vibrational frequency,  $k_B$  is the Boltzmann constant, and  $T$  is the temperature. Mode diffusivity is calculated by

$$D_i = \frac{\pi V^2}{3\hbar^2\omega_i^2} \sum_j^{ \neq i} |S_{ij}|^2 \delta(\omega_i - \omega_j), \quad (3)$$

where  $\delta$  is the Dirac delta function and is approximated by the Lorentzian function as

$$\delta(\omega_i - \omega_j) = \frac{\eta}{\pi[(\omega_i - \omega_j)^2 + \eta^2]}, \quad (4)$$

with  $\eta$  as the broadening parameter.  $S_{ij}$  is the heat current operator:

$$S_{ij} = \frac{\hbar}{2V} \mathbf{v}_{ij}(\omega_i + \omega_j). \quad (5)$$

The velocity operator  $\mathbf{v}_{ij}$  is

$$\mathbf{v}_{ij} = \frac{i}{2\sqrt{\omega_i\omega_j}} \sum_{\alpha, \beta} \sum_{m, \kappa, \kappa'} \frac{\Phi_{\kappa' \kappa}^{\beta \alpha}(0, m)}{\sqrt{m_\kappa m_{\kappa'}}} e_\kappa^{i, \alpha} e_{\kappa'}^{j, \beta} (\mathbf{R}_m + \mathbf{R}_{\kappa \kappa'}), \quad (6)$$

where  $\Phi_{\kappa' \kappa}^{\beta \alpha}(0, m)$  is the non-Hermitian force constants,  $e_\kappa^{i, \alpha}$  is the phonon eigenvector for the  $\kappa$ th atom along the cartesian direction  $\alpha$ ,  $m_\kappa$  is the mass of atom  $\kappa$ ,  $\mathbf{R}_m$  is the position of cell  $m$ , and  $\mathbf{R}_{\kappa \kappa'}$  is the distance between atom  $\kappa$  and atom  $\kappa'$  in a cell.

In the QHGK approximation [12], thermal conductivity is expressed by

$$k^{\alpha \beta} = \frac{1}{V} \sum_{ij} c_{ij} v_{ij}^\alpha v_{ij}^\beta \tau_{ij}, \quad (7)$$

$$c_{ij} = \frac{\hbar\omega_i\omega_j}{T} \frac{f_{0i} - f_{0j}}{\omega_j - \omega_i}, \quad (8)$$

and

$$\tau_{ij} = \frac{\Gamma_i + \Gamma_j}{(\Gamma_i + \Gamma_j)^2 + (\omega_i - \omega_j)^2} + O(\varepsilon^2). \quad (9)$$

$f_{0i}$  is the Bose-Einstein occupation number of the  $i$ th normal mode.  $\Gamma_i$  is the linewidth of mode  $i$ , which is related to the lifetime by

$$\tau_i = \frac{1}{2\Gamma_i}. \quad (10)$$

In Eq. (7), the summation of terms with  $i = j$  is the autocorrelation contribution to the thermal conductivity, while the summation of terms with  $i \neq j$  is the cross-correlation contribution to the thermal conductivity.

The anharmonic vibrational frequencies and lifetimes are computed using the MD simulation-based normal mode decomposition (NMD) method [13–15]. In NMD, the trajectories of each atom from MD simulations are projected onto the normal mode:

$$Q(\mathbf{k}, \nu, t) = \sum_{\alpha}^3 \sum_j^n \sum_l^N \sqrt{\frac{m_j}{N}} u_{jl}^{\alpha}(t) e_j^{\alpha*}(\mathbf{k}, \nu) \exp(-i\mathbf{k} \cdot \mathbf{r}_{lj}), \quad (11)$$

where  $N$  is the total number of unit cells,  $m_j$  is the mass of atom  $j$ ,  $u$  is the displacement, and  $e$  is the phonon eigenvector. The spectral energy density (SED) is calculated through the Fourier transform of the time derivative of the normal mode:

$$\Phi(\mathbf{k}, \nu, \omega) = |\mathcal{F}(\dot{Q}(\mathbf{k}, \nu, t))|^2 = \left| \int_0^{+\infty} \dot{Q}(\mathbf{k}, \nu, t) e^{-i\omega t} dt \right|^2. \quad (12)$$

The anharmonic vibrational frequencies and lifetimes are obtained through fitting the SED by a Lorentzian function:

$$\Phi(\mathbf{k}, \nu, \omega) = \frac{C(\mathbf{k}, \nu)}{[\omega - \omega^A(\mathbf{k}, \nu)]^2 + [\Gamma(\mathbf{k}, \nu)]^2}, \quad (13)$$

where  $\omega$  is the spectral frequency,  $\omega^A$  is the anharmonic frequency, and  $\Gamma$  is the linewidth.

For  $a\text{-SiO}_2$ , the atomic structure is disordered. Therefore, the NMD is carried out only at the gamma point ( $\mathbf{k} = 0$ ).

### III. COMPUTATIONAL DETAILS

MD simulation is a versatile tool to investigate thermal transport [16,17]. The open-source package LAMMPS [18] is used to perform MD simulations of  $a\text{-SiO}_2$ . The vibrational properties and thermal conductivities are computed based on MD simulations. The van Beest-Krammer-van Santen (BKS) potential modified by adding a 24–6 Lennard-Jones (LJ) potential [19–21] is employed. The cutoffs of Buckingham and LJ potentials are set to 10 Å and 8.5 Å, respectively. The electrostatic interactions are calculated through the Wolf summation method with a cutoff of 12 Å and a damping factor of 0.223 Å<sup>-1</sup>.

All simulations are carried out with periodic boundary conditions and a time step of 0.905 fs. This time step is chosen according to the work of Larkin and McGaughey [22], which also studies the thermal conductivity of  $a\text{-SiO}_2$  using the modified BKS potential. Good thermostat is reached using this time step. The melt-quench procedure is used to obtain the atomic configurations of  $a\text{-SiO}_2$  at different temperatures [23]. First, a system containing 648 atoms for  $a\text{-SiO}_2$  is melted to 8000 K in a constant number, pressure, and temperature (NPT) ensemble. Then, the system is cooled at a rate of 2.21 ~ 3.37 K/ps to 1900 K, 1500 K, 1300 K, 1100 K, 900 K, 700 K, 500 K, 300 K, 200 K, and 100 K. When cooled to 1100 K,  $a\text{-SiO}_2$  is annealed in a NPT ensemble for 9 ns to remove metastability before continuing the cooling [22]. After the cooling process, the system is further equilibrated in a NPT ensemble for 1.8 ns, followed by a constant number, volume, and temperature (NVT) ensemble for 0.9 ns, and then a constant number, volume, and energy (NVE) ensemble for 0.9 ns.

The radial distribution function (RDF) of  $a\text{-SiO}_2$  is calculated as shown in Fig. 1 in comparison with the RDF of  $a\text{-SiO}_2$  from previous MD simulations [22] and experimental data [24]. The results from this work are in good agreement with previous work. The first nearest neighbors for Si-O, O-O, and Si-Si are 1.62 Å, 2.58 Å, and 3.06 Å, respectively, which compare well with the experimental measurements of 1.60 Å, 2.60 Å, and 3.05 Å [24].

To calculate the thermal conductivities through the Green-Kubo formula, the time step is set to 0.2 fs. The MD simulations are carried out for 8 ns in a NVE ensemble, during which the autocorrelation function of the heat flux is calculated every 2 fs. The thermal conductivity is obtained by integrating the autocorrelation function of the heat flux.

To perform the NMD, the equilibrium configuration of  $a\text{-SiO}_2$  is first obtained through energy minimization. After the minimization, the system is equilibrated with a time step of 0.2 fs in a NVT ensemble for 0.2 ns at the targeted temper-

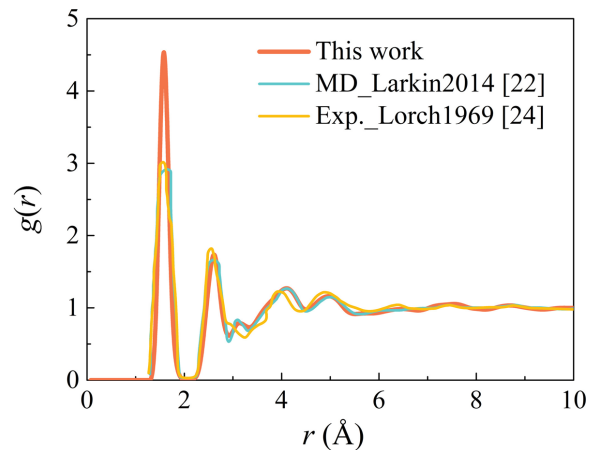


FIG. 1. Radial distribution function  $g(r)$  of  $a\text{-SiO}_2$  of all atom pairs at 300 K from this work, MD simulations of Larkin and McGaughey [22], and experimental measurement [24].

ature, and then in a NVE ensemble for an additional 0.2 ns. After the equilibrium process, the velocities of each atom are dumped every 5 fs in a NVE ensemble during a time span of 1 ns for postprocessing.

Force constants are calculated by the General Utility Lattice Program [25] based on the equilibrium configurations of  $a\text{-SiO}_2$ . Then, the harmonic vibrational properties are obtained through lattice dynamics calculations using the PHONOPY code [26].

### IV. VIBRATIONAL MODE PROPERTIES

The IPR and phonon DOS are computed as shown in Fig. 2. The equation for calculating the IPR is

$$\frac{1}{p(\mathbf{k}, \nu)} = \sum_j \left[ \sum_{\alpha} (e_j^{\alpha}(\mathbf{k}, \nu))^2 \right]^2, \quad (14)$$

where  $e_j^{\alpha}$  is the eigenvector of atom  $j$  along the direction  $\alpha$ . The IPR characterizes the extent of localization for a specific mode. For the vibration localized on a single atom,

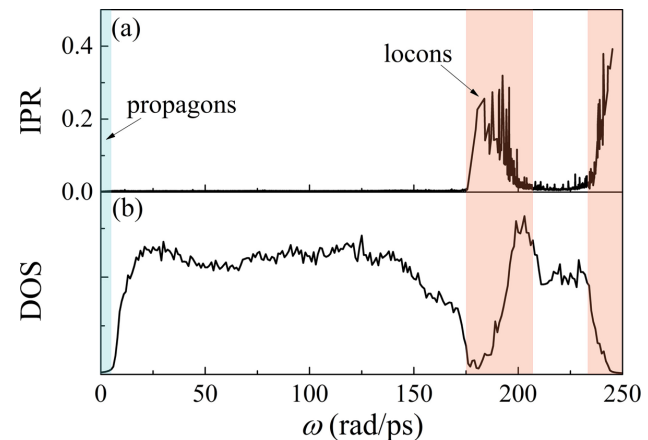


FIG. 2. The inverse participation ratio and density of states of vibrational modes in  $a\text{-SiO}_2$  at 300 K.

$1/p$  would be 1, while  $1/p$  would be  $1/N$  if the vibrations were equally distributed on all atoms. Figure 2(a) indicates that locons are located in two frequency regions, 175 to 206 rad/ps and more than 234 rad/ps, which are shaded in light red. The other modes are delocalized, including propagons and diffusons. Larkin and McGaughey [22] have reported a propagons/diffusons cutoff frequency of 4.55 rad/ps. Here we use the same cutoff frequency. The frequency region of propagons is shaded in light blue in Fig. 2, and the frequency region of diffusons is not shaded. These results indicate that diffusons are the dominate vibrational modes in  $a\text{-SiO}_2$ . Due to the limited size of our simulated system, the lowest frequency predicted in this work is 7.31 rad/ps. Therefore, only diffusons and locons are considered in this work. This is reasonable because the contribution of propagons to the total thermal conductivity of  $a\text{-SiO}_2$  is negligible according to previous investigations [22].

The DOS is calculated by

$$\text{DOS}(\omega) = \sum_i \delta(\omega_i - \omega), \quad (15)$$

and is plotted in Fig. 2(b). For diffusons, the DOS is constant over most of the frequency range. The DOS of locons increases with frequency in the range of 175 to 206 rad/ps, and decreases with frequency in the range of 234 to 245 rad/ps. Locons only constitute approximately 10% of the total vibrational modes.

Next, we move to investigate the effect of anharmonicity on phonon vibrational spectra. The anharmonic vibrational frequencies and lifetimes at different temperatures are calculated through the NMD method described in Sec. II. The density of states at different temperatures are shown in Fig. 3(a). The anharmonicity leads to a red shift in the vibrational frequency, and the shift increases with an increase in temperature. Lv and Henry [10] also reported a lowering in the vibrational frequencies of  $a\text{-SiO}_2$  at higher temperatures. The frequency shift, which is the difference between the anharmonic vibrational frequency and harmonic vibrational frequency, is plotted in Fig. 3(b). At 100 K, the frequency shift is small and oscillates around zero. When the temperature increases to 300 K, the frequency shifts of most modes become negative. With an increase in temperature, the negative frequency shift becomes larger. The frequency shifts of locons are, in general, larger than diffusons. This indicates that anharmonicity has a more pronounced influence on locons than diffusons.

The anharmonicity-induced frequency shifts are less than 10% for 99.6% vibrational modes. Therefore, it is appropriate to use the QHGK expression derived by Isaeva *et al.* [12] and replace the frequency in QHGK by the temperature-dependent frequencies.

The vibrational mode lifetimes are plotted in Fig. 4. The lifetimes of diffusons first decrease and then increase with frequency. A local peak forms at the diffusons/locons cutoff frequency (175 rad/ps). With the increase in temperature, the lifetimes decrease due to the anharmonic effect.

## V. COMPARISON BETWEEN AF THEORY AND QHGK

The anharmonic effect on the thermal conductivities of  $a\text{-SiO}_2$  can be investigated at two levels. First, one can com-

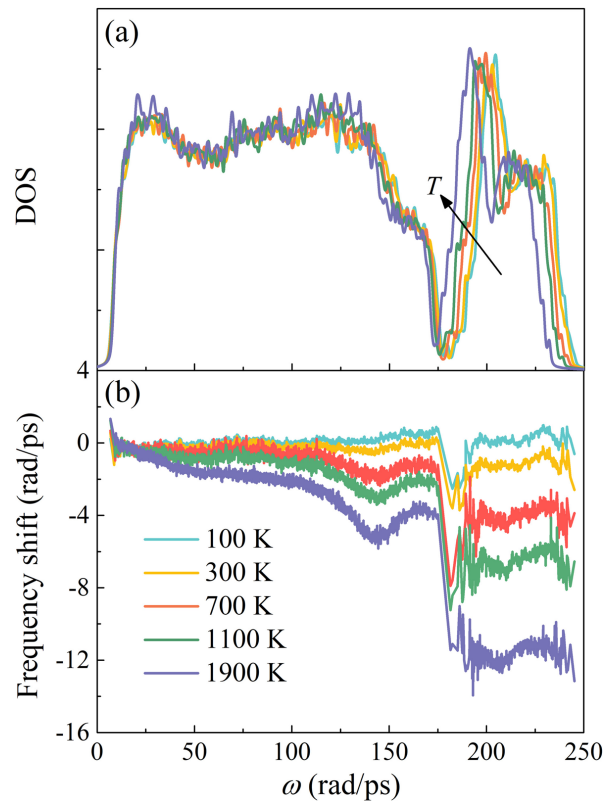


FIG. 3. (a) The DOS of anharmonic vibrational modes at different temperatures. (b) Frequency shifts at different temperatures.

pare the results from AF theory and QHGK. AF theory was derived based on harmonic approximation, which can only be used for predicting the thermal conductivities of stiff material at low temperatures [6]. QHGK is applicable to systems with anharmonicity at higher temperatures due to the introduction of vibrational lifetimes [12]. Second, since the vibrational frequencies change with temperature due to anharmonicity, using temperature-dependent frequencies allows us to consider the anharmonic effect more accurately. In this section, we compare the results of AF theory and QHGK.

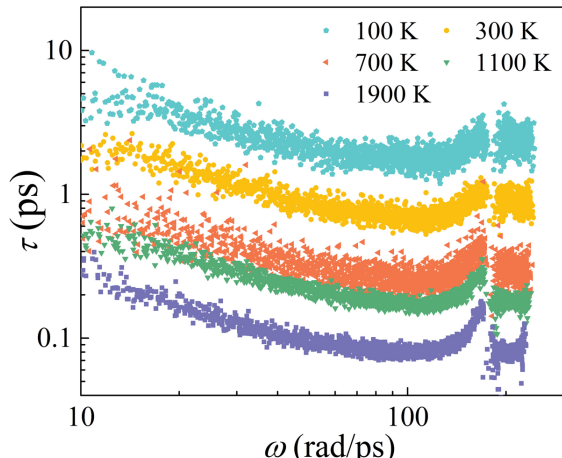


FIG. 4. The vibrational mode lifetimes of  $a\text{-SiO}_2$  at different temperatures.

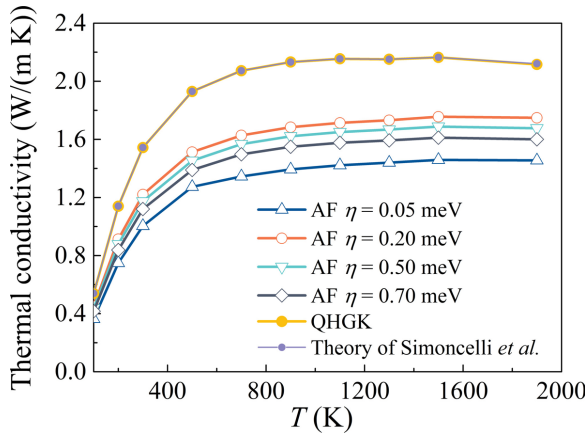


FIG. 5. The thermal conductivities calculated by AF theory [6], QHGK [12], and the theory of Simoncelli *et al.* [11] using harmonic vibrational frequencies.  $\eta$  is the broadening parameter in the AF theory.

In the next section, the thermal conductivities calculated using temperature-dependent frequencies will be compared with those calculated using harmonic frequencies.

The result of AF theory [Eqs. (1)–(6)] is sensitive to the choice of the broadening parameter  $\eta$ . The effect of  $\eta$  on thermal conductivity is shown in Fig. 5. With an increase in  $\eta$ , thermal conductivity first increases to a peak value at  $\eta = 0.2$  meV, and then decreases. The maximum thermal conductivities predicted by AF theory are lower than those calculated by QHGK in the whole temperature range. This result indicates that more careful consideration of anharmonicity in the model leads to an increase in the thermal conductivities. With an increase in temperature, the difference between the results of QHGK and AF theory increase followed by a slight decrease, as shown by the triangles in Fig. 6.

The thermal conductivities of *a*-SiO<sub>2</sub> are also calculated by the anharmonic theory derived by Simoncelli *et al.* [11], as shown by the purple circles in Fig. 5. The results of QHGK

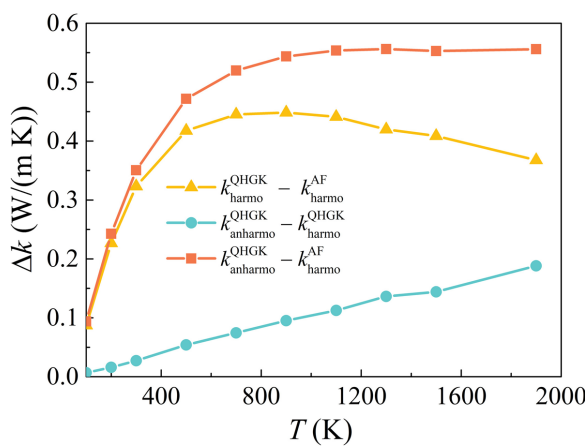


FIG. 6. The difference between the thermal conductivities calculated by different methods.  $k_{\text{QHGK}}^{\text{harmo}}$  is the thermal conductivity calculated by QHGK using harmonic vibrational frequencies.  $k_{\text{harmo}}^{\text{AF}}$  is the thermal conductivity calculated by AF theory using harmonic vibrational frequencies.  $k_{\text{anharmo}}^{\text{QHGK}}$  is the thermal conductivity calculated by QHGK using anharmonic vibrational frequencies.

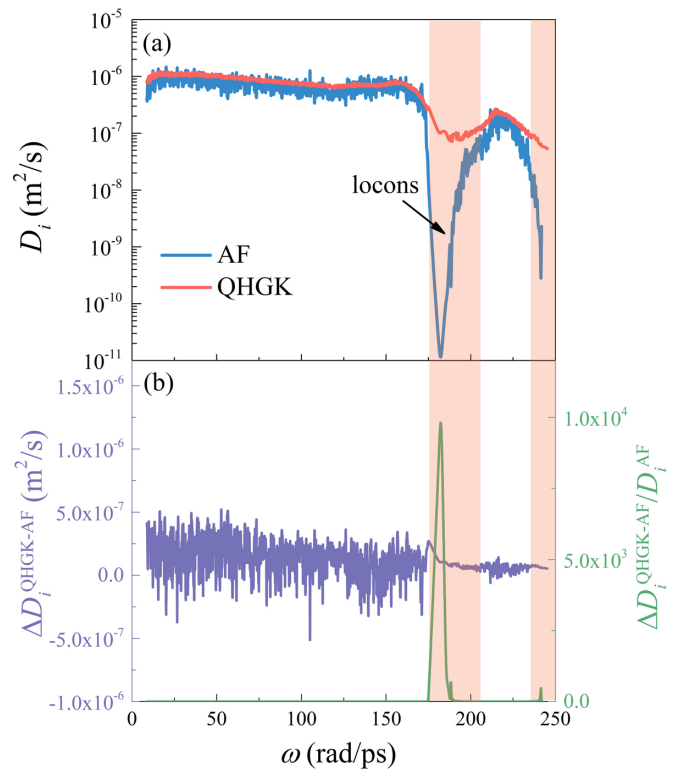


FIG. 7. (a) The diffusivities of vibrational modes in *a*-SiO<sub>2</sub> at 1900 K calculated by AF theory [Eq. (16)] and QHGK [Eq. (17)]. (b) The absolute (left) and relative (right) differences between the diffusivities calculated by QHGK and AF theory.

[12] are in agreement with the results of the theory of Simoncelli *et al.* [11].

The classical AF theory and QHGK can both be written in the form of Eq. (1) with  $C_i = k_B$ . Therefore, the difference between the thermal conductivities calculated by these two models lies in the difference in the diffusivities. The mode diffusivities of AF theory and QHGK can be expressed by

$$D_i^{\text{AF}} = \frac{1}{3} \sum_j^{\neq i} D_{ij}^{\text{AF}} = \frac{1}{3} \sum_j^{\neq i} |v_{ij}|^2 \left[ \frac{\pi}{4} \left( \frac{\omega_j}{\omega_i} + 1 \right)^2 \right] \delta(\omega_j - \omega_i) \quad (16)$$

and

$$D_i^{\text{QHGK}} = \frac{1}{3} \sum_j D_{ij}^{\text{QHGK}} = \frac{1}{3} \sum_j |v_{ij}|^2 \tau_{ij}, \quad (17)$$

respectively.

The comparison between the mode diffusivities of AF theory and QHGK is shown in Fig. 7(a). The diffusivities computed by QHGK are generally larger than the diffusivities calculated by AF theory. The absolute and relative differences between the diffusivities calculated by these two theories are  $\Delta D_i^{\text{QHGK-AF}} = D_i^{\text{QHGK}} - D_i^{\text{AF}}$  and  $\Delta D_i^{\text{QHGK-AF}} / D_i^{\text{AF}}$ , respectively, as shown in Fig. 7(b).  $\Delta D_i^{\text{QHGK-AF}}$  of diffusons (4.55 to 175 rad/ps and 206 to 234 rad/ps) is generally larger than  $\Delta D_i^{\text{QHGK-AF}}$  of locons (175 to 206 rad/ps and more than 234 rad/ps). However,  $\Delta D_i^{\text{QHGK-AF}} / D_i^{\text{AF}}$  of diffusons is

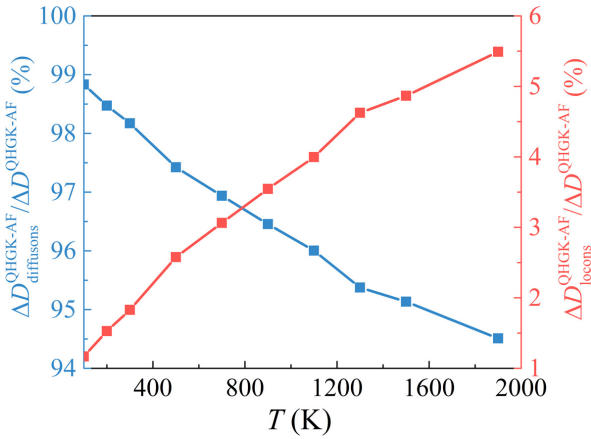


FIG. 8. The temperature dependence of the relative contributions of diffusons (left) and locons (right) to the total diffusivity difference between QHGK and AF theory.

much smaller than  $\Delta D_i^{\text{QHGK-AF}}/D_i^{\text{AF}}$  of locons. The relative contributions of diffusons and locons to the total diffusivity difference are calculated by

$$\frac{\Delta D_{\text{diffusons}}^{\text{QHGK-AF}}}{\Delta D^{\text{QHGK-AF}}} = \frac{\sum_i^{\text{diffusons}} (D_i^{\text{QHGK}} - D_i^{\text{AF}})}{\sum_i^{\text{total}} (D_i^{\text{QHGK}} - D_i^{\text{AF}})} \quad (18)$$

and

$$\frac{\Delta D_{\text{locons}}^{\text{QHGK-AF}}}{\Delta D^{\text{QHGK-AF}}} = \frac{\sum_i^{\text{locons}} (D_i^{\text{QHGK}} - D_i^{\text{AF}})}{\sum_i^{\text{total}} (D_i^{\text{QHGK}} - D_i^{\text{AF}})}, \quad (19)$$

respectively. The variations of  $\Delta D_{\text{diffusons}}^{\text{QHGK-AF}}/\Delta D^{\text{QHGK-AF}}$  and  $\Delta D_{\text{locons}}^{\text{QHGK-AF}}/\Delta D^{\text{QHGK-AF}}$  with temperatures are plotted in Fig. 8. The relative contributions of diffusons to the total diffusivity difference are 94% to 99%, while the relative contributions of locons are only 1.0% to 5.5%. With the increase in temperature,  $\Delta D_{\text{diffusons}}^{\text{QHGK-AF}}/\Delta D^{\text{QHGK-AF}}$  decreases, while  $\Delta D_{\text{locons}}^{\text{QHGK-AF}}/\Delta D^{\text{QHGK-AF}}$  increases. These results indicate that although the anharmonicity has a greater influence on locons than diffusons, the increase in diffusivities and thermal conductivities caused by the anharmonicity are mostly contributed by the anharmonic diffusons. This is because the diffusons account for 90% of the total vibrational modes, and the diffusivities of diffusons are much larger than the diffusivities of locons.

## VI. EFFECT OF ANHARMONIC VIBRATIONAL FREQUENCIES ON THERMAL CONDUCTIVITY

Due to anharmonicity, vibrational frequencies decrease with an increase in temperature, as shown in Fig. 3. The use of temperature-dependent frequencies (anharmonic frequencies) allows us to consider the anharmonic effect more accurately. A comparison is made between the thermal conductivities calculated using harmonic and anharmonic frequencies, and the results are plotted in Fig. 9. The blue line shows the thermal conductivity computed by QHGK using harmonic frequencies and classical specific heat, while the yellow line is the thermal conductivity computed by QHGK using anhar-

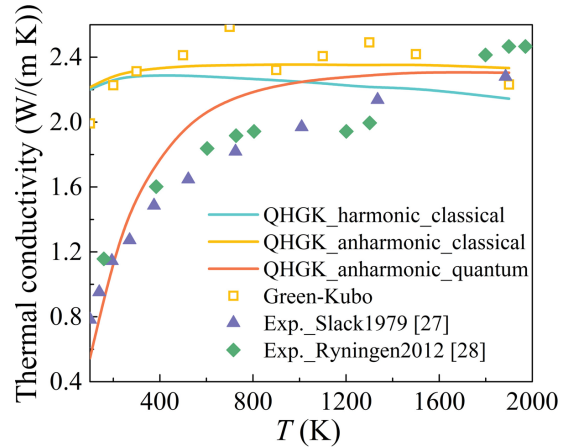


FIG. 9. The thermal conductivities calculated by QHGK using harmonic or anharmonic vibrational frequencies and classical or quantum specific heat, and their comparisons with the results of the Green-Kubo formula based on MD simulations and experimental data [27,28].

monic frequencies and classical specific heat. The thermal conductivities calculated using anharmonic frequencies are higher than those calculated using harmonic frequencies at all temperatures. This result indicates that the anharmonicity-induced frequency shifts have a positive contribution to the thermal conduction in  $a\text{-SiO}_2$ . The difference between the thermal conductivities calculated using anharmonic frequencies and harmonic frequencies increases with temperature, as shown by the circles in Fig. 6. The total changes in the thermal conductivity induced by the anharmonicity introduced in QHGK and the anharmonic frequencies increase monotonically with temperature, as shown by the squares in Fig. 6.

The comparisons between the thermal conductivities calculated by different methods shown in Fig. 9 also reveal the mechanisms for the positive temperature dependence of the thermal conductivity of  $a\text{-SiO}_2$ . If the harmonic frequencies and classical specific heat were used, the thermal conductivity decreases at high temperatures (blue line in Fig. 9). The thermal conductivity increases at high temperatures after the use of the anharmonic frequencies (yellow line in Fig. 9). This indicates that the anharmonicity-induced temperature dependence of the vibrational frequencies is a mechanism for the positive temperature dependence of the thermal conductivity. Considering the quantum specific heat in the theory leads to a steeper temperature dependence of the thermal conductivity (orange line in Fig. 9), which is in reasonable agreement with experimental data [27,28].

Furthermore, the thermal conductivities of  $a\text{-SiO}_2$  are calculated by the Green-Kubo formula based on MD simulations (yellow squares in Fig. 9) for comparison. The heat flux calculated by MD simulations can consider a full order of anharmonicity. The difference between the thermal conductivity calculated by QHGK and MD simulation-based Green-Kubo is within 15%. This comparison is a verification of the theory of QHGK with anharmonic frequencies as an appropriate method for calculating the thermal conductivity of  $a\text{-SiO}_2$  considering anharmonicity.

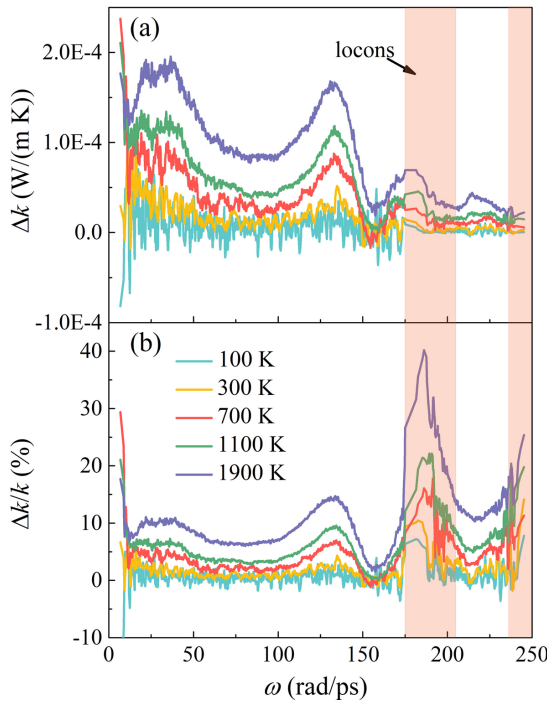


FIG. 10. The absolute (a) and relative (b) changes in the thermal conductivity of different modes induced by frequency shifts.

The absolute  $\Delta k$  and relative changes  $\Delta k/k$  in the thermal conductivity of different modes induced by frequency shifts are shown in Fig. 10(a) and 10(b), respectively. With the increase in temperature, both  $\Delta k$  and  $\Delta k/k$  increase, which corresponds to the increase of the negative frequency shift [Fig. 3(b)]. This result indicates a positive correlation between the negative frequency shift and the changes in the thermal conductivity. However,  $\Delta k$  of diffusons is larger than  $\Delta k$  of locons [Fig. 10(a)], while the frequency shifts of diffusons are smaller than locons. This is because  $\Delta k$  is also influenced by the mode diffusivity. The diffusivity of diffusons is larger than locons, as shown in Fig. 11(a), thus resulting in the larger absolute changes in the thermal conductivity.  $\Delta k/k$  of locons are larger than  $\Delta k/k$  of diffusons (Fig. 10(b)), which agrees with the larger frequency shifts of locons [Fig. 3(b)].

The mode diffusivities computed using harmonic and anharmonic frequencies are compared as shown in Fig. 11(a). Anharmonic diffusivity is larger than harmonic diffusivity for all vibrational modes. The absolute and relative differences between the anharmonic and harmonic diffusivities are  $\Delta D_i^{\text{anharmo-harmo}} = D_i^{\text{anharmo}} - D_i^{\text{harmo}}$  and  $\Delta D_i^{\text{anharmo-harmo}} / D_i^{\text{harmo}}$ , respectively, as shown in Fig. 11(b).  $\Delta D_i^{\text{anharmo-harmo}}$  of diffusons is generally larger than  $\Delta D_i^{\text{anharmo-harmo}}$  of locons, while  $\Delta D_i^{\text{anharmo-harmo}} / D_i^{\text{harmo}}$  of locons is larger than  $\Delta D_i^{\text{anharmo-harmo}} / D_i^{\text{harmo}}$  of diffusons. The relative contributions of diffusons and locons to the total diffusivity difference are calculated by

$$\frac{\Delta D_i^{\text{anharmo-harmo}}}{\Delta D_i^{\text{anharmo-harmo}}} = \frac{\sum_i^{\text{diffusons}} (D_i^{\text{anharmo}} - D_i^{\text{harmo}})}{\sum_i^{\text{total}} (D_i^{\text{anharmo}} - D_i^{\text{harmo}})} \quad (20)$$

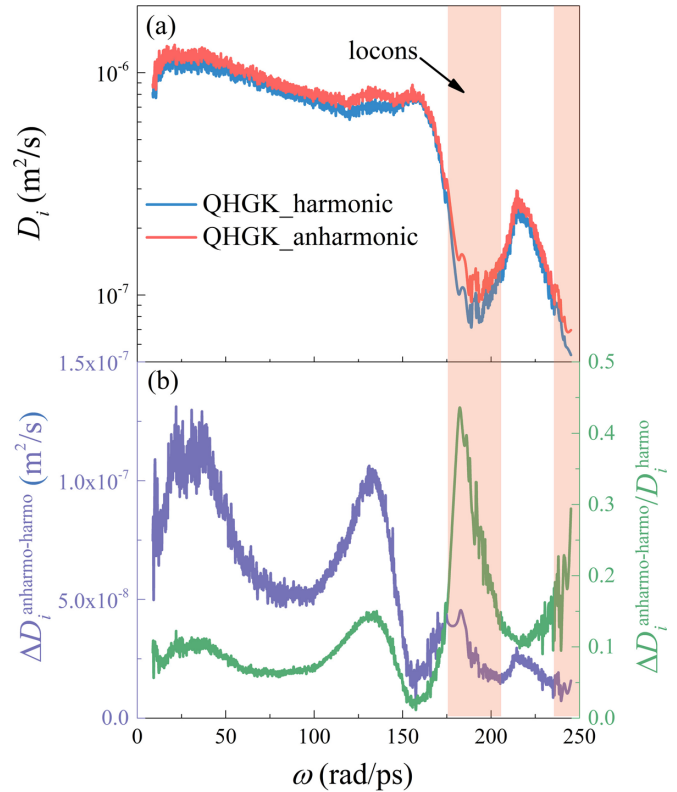


FIG. 11. (a) The diffusivities of vibrational modes in  $a\text{-SiO}_2$  at 1900 K calculated by QHGK [Eq. (17)] using harmonic and anharmonic vibrational frequencies, respectively. (b) The absolute (left) and relative (right) differences between diffusivities calculated using anharmonic and harmonic vibrational frequencies.

and

$$\frac{\Delta D_{\text{locons}}^{\text{anharmo-harmo}}}{\Delta D_{\text{anharmo-harmo}}} = \frac{\sum_i^{\text{locons}} (D_i^{\text{anharmo}} - D_i^{\text{harmo}})}{\sum_i^{\text{total}} (D_i^{\text{anharmo}} - D_i^{\text{harmo}})}, \quad (21)$$

respectively. The variations of  $\Delta D_{\text{diffusons}}^{\text{anharmo-harmo}} / \Delta D_{\text{anharmo-harmo}}$  and  $\Delta D_{\text{locons}}^{\text{anharmo-harmo}} / \Delta D_{\text{anharmo-harmo}}$  with temperature are shown in Fig. 12.  $\Delta D_{\text{diffusons}}^{\text{anharmo-harmo}}$  accounts for 97% to 99% of the total diffusivity difference, while  $\Delta D_{\text{locons}}^{\text{anharmo-harmo}}$  only accounts for 1.0% to 3.0%. With an increase in temperature,  $\Delta D_{\text{diffusons}}^{\text{anharmo-harmo}} / \Delta D_{\text{anharmo-harmo}}$  decreases, while  $\Delta D_{\text{locons}}^{\text{anharmo-harmo}} / \Delta D_{\text{anharmo-harmo}}$  increases. These results indicate that the increase of the diffusivities and thermal conductivities induced by the anharmonicity-induced frequency shifts is mostly contributed by the anharmonic diffusons, while the anharmonicity has a larger influence on locons than diffusons.

To investigate the mechanism for the heat transfer in  $a\text{-SiO}_2$  further, the contributions of autocorrelation and cross-correlation of diffusons and locons to the thermal conductivity are calculated. It is found that the autocorrelations of both diffusons and locons are zero. The contributions of cross-correlations of diffusons–diffusons, diffusons–locons, and locons–locons to the total thermal conductivities are plotted in Fig. 13. The cross-correlations between diffusons and diffusons, and between diffusons and locons, contribute 97.37% ~ 99.99% and 0.01% ~ 2.22% to the total thermal conductivity, respectively. The cross-correlations between locons

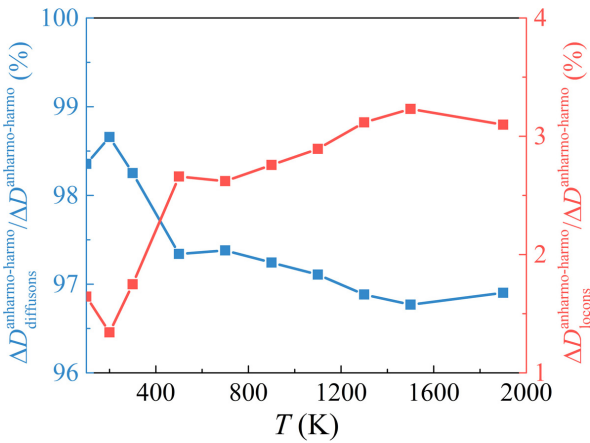


FIG. 12. The temperature dependence of the relative contributions of diffusons (left) and locons (right) to the total difference between the diffusivities calculated by anharmonic and harmonic vibrational frequencies.

and locons are negligible. These results indicate that heat is transferred in  $\alpha\text{-SiO}_2$  mainly through the interaction between diffusons and diffusons. Locons contribute to the heat transfer mainly through collaboration with diffusons.

The effects of anharmonicity on the thermal conductivity of  $\alpha\text{-SiO}_2$  are summarized in Fig. 14. QHGK with anharmonic vibrational frequencies can well reproduce the experimental value. However, QHGK ignoring anharmonicity-induced frequency shifts underestimates the thermal conductivity by 8.17%. Compared to QHGK, AF theory underestimates the thermal conductivity by 14.09% or 24.13%, depending on whether anharmonicity-induced frequency shifts are considered or not considered. Figure 14 also shows that diffusons–diffusons cross-correlations dominate the heat conduction in  $\alpha\text{-SiO}_2$ , and consideration of anharmonicity in the thermal conductivity model (QHGK) enhances the contribution of diffusons–locons cross-correlations to the thermal conductivity.

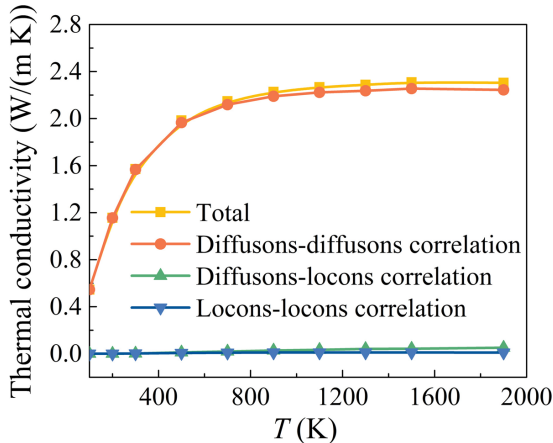


FIG. 13. The contributions of cross-correlations between diffusons and diffusons, between diffusons and locons, and between locons and locons to the total thermal conductivity.

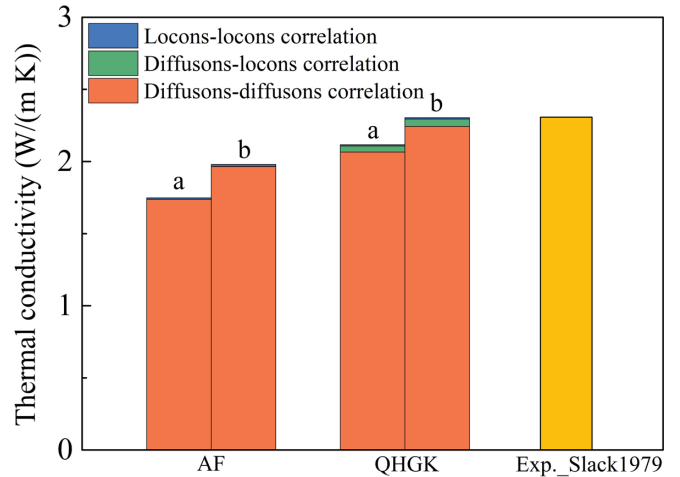


FIG. 14. Thermal conductivity of  $\alpha\text{-SiO}_2$  at 1900 K computed by AF theory and QHGK, and a comparison with experimental data [27]. The symbol a represents the results calculated using harmonic vibrational frequencies, while b represents the results calculated using anharmonic vibrational frequencies.

## VII. CONCLUSION

We investigated the effect of anharmonicity on thermal conduction in  $\alpha\text{-SiO}_2$  from two perspectives. First, a comparison is made between QHGK and AF theory. QHGK is a thermal conductivity model that can consider both anharmonicity and disorder. AF theory is also applicable to amorphous materials, but it ignores the effects of anharmonicity in the atomic interactions. It is found that the thermal conductivities calculated by QHGK are larger than the predictions of AF theory. Second, a comparison is made between thermal conductivities calculated using anharmonic and harmonic vibrational frequencies. It is found that the use of anharmonic vibrational frequencies results in a higher thermal conductivity compared with that calculated using harmonic vibrational frequencies. The temperature dependence of the anharmonic vibrational frequencies is a mechanism for the positive temperature dependence of thermal conductivity. Further investigation of mode diffusivities indicates that the enhancement of the thermal conductivity due to the anharmonicity is mainly contributed by the anharmonic diffusons, though the anharmonicity has a larger influence on locons than diffusons. This is because diffusons have larger mode diffusivities than locons, and diffusons constitute 90% of the total vibrational modes. Finally, it is found that cross-correlation between diffusons and diffusons is the major mechanism for heat conduction in  $\alpha\text{-SiO}_2$ , and locons transfer the heat mainly through collaboration with diffusons.

## ACKNOWLEDGMENTS

The authors gratefully thank Prof. Hua Bao at Shanghai Jiao Tong University for many insightful suggestions and revisions of this manuscript.

This work was supported by the National Natural Science Foundation of China (Grant No. 12005019).

- [1] V. Murashov and M. A. White, in *Thermal Conductivity: Theory, Properties, and Applications*, edited by T. M. Tritt, (Kluwer Academic/Plenum Publishers, New York, 2004), p. 93.
- [2] A. I. Krivchikov and A. Jeżowski, Thermal conductivity of glasses and disordered crystals, [arXiv:2011.14728](#).
- [3] S. Alexander, C. Laermans, R. Orbach, and H. M. Rosenberg, Fracton interpretation of vibrational properties of cross-linked polymers, glasses, and irradiated quartz, *Phys. Rev. B* **28**, 4615 (1983).
- [4] S. Alexander, O. Entin-Wohlman, and R. Orbach, Phonon-fracton anharmonic interactions: The thermal conductivity of amorphous materials, *Phys. Rev. B* **34**, 2726 (1986).
- [5] A. Jagannathan, R. Orbach, and O. Entin-Wohlman, Thermal conductivity of amorphous materials above the plateau, *Phys. Rev. B* **39**, 13465 (1989).
- [6] P. B. Allen and J. L. Feldman, Thermal conductivity of disordered harmonic solids, *Phys. Rev. B* **48**, 12581 (1993).
- [7] J. L. Feldman, M. D. Kluge, P. B. Allen, and F. Wooten, Thermal conductivity and localization in glasses: Numerical study of a model of amorphous silicon, *Phys. Rev. B* **48**, 12589 (1993).
- [8] S. Shenogin, A. Bodapati, P. Kebinski, and A. J. H. McGaughey, Predicting the thermal conductivity of inorganic and polymeric glasses: The role of anharmonicity, *J. Appl. Phys.* **105**, 034906 (2009).
- [9] W. Lv and A. Henry, Direct calculation of modal contributions to thermal conductivity via Green-Kubo modal analysis, *New J. Phys.* **18**, 013028 (2016).
- [10] W. Lv and A. Henry, Non-negligible contributions to thermal conductivity from localized modes in amorphous silicon dioxide, *Sci. Rep.* **6**, 35720 (2016).
- [11] M. Simoncelli, N. Marzari, and F. Mauri, Unified theory of thermal transport in crystals and glasses, *Nat. Phys.* **15**, 809 (2019).
- [12] L. Isaeva, G. Barbinalardo, D. Donadio, and S. Baroni, Modeling heat transport in crystals and glasses from a unified lattice-dynamical approach, *Nat. Commun.* **10**, 3853 (2019).
- [13] M. T. Dove, *Introduction to Lattice Dynamics* (Cambridge University Press, Cambridge, 1993).
- [14] A. J. H. McGaughey and J. M. Larkin, Predicting phonon properties from equilibrium molecular dynamics simulations, *Annu. Rev. Heat Transfer* **17**, 49 (2014).
- [15] C. Shao and J. Shiomi, Negligible contribution of inter-dot coherent modes to heat conduction in quantum-dot superlattice, *Mater. Today Phys.* **22**, 100601 (2022).
- [16] D. K. Ma, X. Wan, and N. Yang, Unexpected thermal conductivity enhancement in pillared graphene nanoribbon with isotopic resonance, *Phys. Rev. B* **98**, 245420 (2018).
- [17] L. K. Lu, D. K. Ma, M. Zhong, and L. F. Zhang, Temperature oscillation in one-dimensional superlattice induced by phonon localization, *New J. Phys.* **24**, 013007 (2022).
- [18] S. Plimpton, Fast parallel algorithms for short-range molecular dynamics, *J. Comput. Phys.* **117**, 1 (1995).
- [19] B. W. H. van Beest, G. J. Kramer, and R. A. van Santen, Force Fields for Silicas and Aluminophosphates Based on *Ab Initio* Calculations, *Phys. Rev. Lett.* **64**, 1955 (1990).
- [20] Y. Guissani and B. Guillot, A numerical investigation of the liquid–vapor coexistence curve of silica, *J. Chem. Phys.* **104**, 7633 (1996).
- [21] A. J. H. McGaughey and M. Kaviani, Thermal conductivity decomposition and analysis using molecular dynamics simulations: Part II. Complex silica structures, *Int. J. Heat Mass Transfer* **47**, 1799 (2004).
- [22] J. M. Larkin and A. J. H. McGaughey, Thermal conductivity accumulation in amorphous silica and amorphous silicon, *Phys. Rev. B* **89**, 144303 (2014).
- [23] C. Shao and H. Bao, A molecular dynamics investigation of heat transfer across a disordered thin film, *Int. J. Heat Mass Transfer* **85**, 33 (2015).
- [24] E. Lorch, Neutron diffraction by germania, silica and radiation-damaged silica glasses, *J. Phys. C Solid State Phys.* **2**, 229 (1969).
- [25] J. D. Gale and A. L. Rohl, The general utility lattice program (GULP), *Mol. Simul.* **29**, 291 (2003).
- [26] A. Togo and I. Tanaka, First principles phonon calculations in materials science, *Ser. Mater.* **108**, 1 (2015).
- [27] G. A. Slack, in *Solid State Physics*, edited by H. Ehrenreich, F. Seitz, and D. Turnbull (Academic Press, Cambridge, 1979), p. 1.
- [28] B. Ryninen, M. P. Bellmann, R. Kvande, and O. Lohne, in *27th European Photovoltaic Solar Energy Conference and Exhibition*, edited by S. Nowak, A. Jäger-Waldau, and P. Helm (WIP, Munich, 2012), p. 926.